New Journal of Physics
The open-access journal for physics

3D electron fluid turbulence at nanoscales in dense plasmas

Dastgeer Shaikh[1] **and P K Shukla**[2,3,4,5,6]

[1] Center for Space Plasma and Aeronomy Research, The University of Alabama in Huntsville, Huntsville, AL 35899, USA
[2] Institut für Theoretische Physik IV, Ruhr-Universität Bochum, D-44780 Bochum, Germany
[3] Department of Physics, Umeå University, SE-90187 Umeå, Sweden
[4] SUPA Department of Physics, University of Strathclyde, Glasgow G4 0NG, UK
[5] Instituto de Plasmas e Fusão Nuclear, Instituto Superior Técnico, Universidade Técnica de Lisboa, 1049-001 Lisboa, Portugal
E-mail: dastgeer@cspar.uah.edu and ps@tp4.rub.de

New Journal of Physics **10** (2008) 083007 (9pp)
Received 31 March 2008
Published 6 August 2008
Online at http://www.njp.org/
doi:10.1088/1367-2630/10/8/083007

Abstract. We have performed three-dimensional (3D) nonlinear fluid simulations of electron fluid turbulence at nanoscales in an unmagnetized warm dense plasma in which mode coupling between wave function and electrostatic (ES) potential associated with underlying electron plasma oscillations (EPOs) lead to nonlinear cascades in inertial range. While the wave function cascades towards smaller length scales, ES potential follows an inverse cascade. We find from our simulations that the quantum diffraction effect associated with a Bohm potential plays a critical role in determining the inertial range turbulent spectrum and the subsequent transport level exhibited by the 3D EPOs.

Contents

[6] Author to whom any correspondence should be addressed.

© IOP Publishing Ltd and Deutsche Physikalische Gesellschaft

1. Introduction

Studies of collective phenomena at nanoscales in dense matter are of great importance in diverse areas of physics, including the fields of plasmonics [1]–[5], semiconductors [6], nano-electromechanical systems [7], quantum-diodes [8], nanotubes and nanowires [9], quantum free electron lasers [10], as well as astrophysical bodies [11, 12] and intense laser–solid density plasma interaction experiments [13] for x-ray and γ-ray sources. In dense plasmas, the electrons are highly degenerate and quantum mechanical effects (e.g. electron tunneling arising from the finite width of the electron wave function) play an essential role at nanoscales. Since degenerate electrons follow the Fermi–Dirac statistics, there appear a new electron equation of state and new forces involving the quantum Bohm potential [14] and electron-1/2 spin effects [15] in dense quantum plasmas. It then turns out that due to the intrinsic nonlinearities associated with the Fermi pressure law and quantum forces, there exists the possibility of localizing electrostatic (ES) [16, 17] and electromagnetic [18] wave energies at nanoscales in dense quantum plasmas. Here, we report simulation studies of three-dimensional (3D) electron fluid turbulence at nanoscales in an unmagnetized warm dense plasma. It is found that 3D nonlinearly interacting electron plasma oscillations (EPOs) [19] in a dense quantum plasma exhibit nanostructures and associated energy spectra that are markedly different from those reported earlier for the 2D case [17]. Furthermore, we stress that the present 3D turbulence properties of EPOs in our dense quantum plasma are significantly different from those in a classical plasma [20]–[22]. In the latter, strong electron plasma wave turbulence has been studied by invoking parametric interactions [23] and by using either multi-dimensional cubic nonlinear Schrödinger (NLS) equations [21, 22] or Zakharov equations [20], which are different from our 3D-coupled NLS–Poisson equations in dense quantum plasmas.

The reason for the surge in studying numerous nonlinear processes in dense quantum plasmas lies in a hope to transfer information through the localized nanostructures one is able to create and sustain in plasmas. The present work dealing with 3D electron fluid turbulence shares a great deal of knowledge with classical fluid turbulence [24, 25], plasma turbulence [26, 27] and superfluid turbulence involving Bose–Einstein condensates (BECs) [28, 29] in ultracold gases. Both in fluids and plasmas as well as in BECs, one encounters the phenomena of inverse energy cascades in which energy transfer from small scales sustains large-scale circulations/structures in the flow, and results in a steady-state inertial range with power-law scaling, as was originally predicted by Kolmogorov, Kraichnan and Iroshnik [24, 25]. While the dynamical equations depicting inverse cascades in fluids and plasmas are the Navier–Stokes and Charney–Hasegawa–Mima equations [26, 27], the energy cascade scenario in BECs is described by the Gross–Pitaevskii equation [28, 29]. In section 2, we describe model equations governing the dynamical evolution of a 3D dense Fermi quantum plasma. We also present conservation laws admitted by the set of 3D equations. In section 3, nonlinear 3D simulation results describing turbulence in such a system are described. Mode structures and corresponding Kolmogorov-like spectra are also discussed. Turbulence transport is described in section 4 and finally the conclusions are contained in section 5.

2. Model equations

In dense quantum plasmas, the Wigner–Poisson (WP) model has been used to derive a set of quantum hydrodynamic (QHD) equations [30] in the mean field approximation. The

QHD equations include the continuity, momentum and Poisson equations. The quantum nature appears in the electron momentum equation through the pressure term, which requires knowledge of the Wigner distribution for a quantum mixture of electron wave functions, each characterized by an occupation probability satisfying the Pauli exclusion principle. The quantum part of the electron pressure is represented as a quantum force $-\nabla\phi_{\rm B}$, where the Bohm potential is [14] $\phi_{\rm B} = -(\hbar^2/2m_{\rm e}\sqrt{n_{\rm e}})\nabla^2\sqrt{n_{\rm e}}$. Here $\hbar$ is the Planck constant divided by 2π, $m_{\rm e}$ is the electron mass and $n_{\rm e}$ is the electron number density. Defining the effective wave function $\psi = \sqrt{n_{\rm e}(\mathbf{r}, t)}\exp[{\rm i}S(\mathbf{r}, t)/\hbar]$, where $\nabla S(\mathbf{r}, t) = m_{\rm e}\mathbf{u}_{\rm e}(\mathbf{r}, t)$ and $\mathbf{u}_{\rm e}(\mathbf{r}, t)$ is the electron velocity, the electron momentum equation can be represented as an effective NLS equation [31], in which there appears a coupling between the wave function and the ES potential associated with the EPOs. The ES potential is determined from the Poisson equation. We thus have the coupled NLS and Poisson equations, which govern the dynamics of nonlinearly interacting EPOs in a warm dense quantum plasma.

In this paper, we carry out simulations of 3D NLS and Poisson equations in order to understand the properties of 3D electron fluid turbulence (involving nanostructures and associated electron transport) in a warm dense plasma. We find that nonlinear couplings between different scale EPOs are responsible for creating small-scale electron density clumps, whereas the ES potential assumes large-scale structures. The total energy associated with our 3D electron fluid turbulence at nanoscales possesses a characteristic spectrum which is *non*-Kolmogorov-like.

For our 3D electron fluid turbulence studies, we use the NLS–Poisson equations [16, 30]

$$ {\rm i}\sqrt{2H}\frac{\partial\Psi}{\partial t} + H\nabla^2\Psi + \varphi\Psi - |\Psi|^{4/3}\Psi = 0 \tag{1} $$

and

$$ \nabla^2\varphi = |\Psi|^2 - 1, \tag{2} $$

which are valid at zero electron temperature for the Fermi–Dirac equilibrium distribution. In equations (1) and (2), the wave function Ψ is normalized by $\sqrt{n_0}$, the ES potential φ by $k_{\rm B}T_{\rm F}/e$, the time t by the electron plasma period $\Omega_{\rm pe}^{-1}$, and the space $\mathbf{r}$ by the Fermi–Debye radius $\lambda_{\rm D}$. We have introduced the notations $\lambda_{\rm D} = (\epsilon_0 k_{\rm B}T_{\rm F}/n_0e^2)^{1/2} \equiv V_{\rm F}/\Omega_{\rm pe}$ and $\sqrt{H} = \hbar\omega_{\rm pe}/\sqrt{2}k_{\rm B}T_{\rm F}$, where ϵ_0 is the electric permittivity, $k_{\rm B}$ is the Boltzmann constant and the Fermi electron temperature $k_{\rm B}T_{\rm F} = (\hbar^2/2m_{\rm e})(3\pi^2)^{1/3}n_0^{2/3}$, e is magnitude of the electron charge, and $\Omega_{\rm pe} = (n_0e^2/\epsilon_0m_{\rm e})^{1/2}$ is the unperturbed electron plasma frequency. The origin of the various terms in equation (1) is obvious. The first term is due to the electron inertia, the H-term is associated with the quantum diffraction effect involving the Bohm potential, $\varphi\Psi$ comes from the nonlinear coupling between the scalar potential (associated with the space charge electric field resulting from oscillations of the electrons around immobile ions) and the electron wave function, and the fourth term in the left-hand side of (1) is the contribution of the 3D electron pressure ($p_{\rm e} = m_{\rm e}V_{\rm F}^2n_{\rm e}^{5/3}/5n_0^{2/3}$) for the Fermi plasma with a quantum statistical equation of state.

Equations (1) and (2) admit a set of conserved quantities [13]: the number of electrons $N = \int\Psi^2\,{\rm d}V$, the electron momentum $\mathbf{P} = -{\rm i}\int\Psi^*\nabla\Psi\,{\rm d}V$, the electron angular momentum $\mathbf{L} = -{\rm i}\int\Psi^*\mathbf{r}\times\nabla\Psi\,{\rm d}V$ and the total energy $\mathcal{E} = \int[-\Psi^*H\nabla^2\Psi + |\nabla\varphi|^2/2 + (3/5)|\Psi|^{10/3}]\,{\rm d}V$, where ${\rm d}V = {\rm d}x\,{\rm d}y\,{\rm d}z$. In obtaining the total energy $\mathcal{E}$, we used the relation $\partial\mathbf{E}/\partial t = {\rm i}H(\Psi\nabla\Psi* - \Psi*\nabla\Psi)$, where the electric field $\mathbf{E} = -\nabla\varphi$. The conserved quantities are used to maintain the accuracy of the numerical integration of equations (1) and (2). We note that

linearizing the latter one obtains the EPO frequency $\omega = \left(\Omega_{pe}^2 + k^2 V_F^2 + \hbar^2 k^4 / 4m_e^2\right)^{1/2}$, which exhibits the dispersive behavior of the EPOs. In the short wavelength regime characterized by $k^2 \gg 4m_e^2 V_F^2/\hbar^2$, one notices that the dispersion associated with the electron tunneling effect dominates over that involving the quantum statistical electron pressure.

3. Nonlinear 3D simulations of quantum plasmas

We have developed 3D fluid code to investigate nonlinear interactions between multiscale EPOs described by (1) and (2). Our 3D fluid code is based on Fourier expansion of the bases using a fully dealiased pseudospectral numerical scheme [32]. The nonlinear deconvolution of Fourier modes is performed by computing the nonlinear triad interactions $\tilde{f}(\mathbf{x}, t)\tilde{g}(\mathbf{x}, t) = \sum_{\mathbf{k}=\mathbf{k}'-\mathbf{k}''} f(\mathbf{k}', t)g(\mathbf{k}'', t)\delta(\mathbf{k}' - \mathbf{k}'')$ at each time, which survive for only those coupled modes which satisfy the Fourier triad constraint $\mathbf{k} = \mathbf{k}' - \mathbf{k}''$. These nonlinear interactions in Fourier space follow from a Kolmogorov phenomenology of spectral energy transfer, and are mediated predominantly by the neighboring modes. Furthermore, such nonlinear interactions in the local spectral space conserve constants of motion of equations (1) and (2), as presented above. The temporal integration is performed by 4th order Runge–Kutta method. The spectral distribution for turbulent fluctuations is initialized isotropically (no mean fields are assumed) with random phases and amplitudes in Fourier space. The evolution variables use periodic boundary conditions. The initial isotropic turbulent spectrum was chosen close to k^{-2}, with random phases in all three directions. The choice of this (or even a flatter than -2) spectrum treats the turbulent fluctuations on an equal footing and avoids any influence on the dynamical evolution that may be due to the initial spectral nonsymmetry. Note, however, that the local as well as global mean flows may subsequently be generated by self-consistently excited nonlinear instabilities. Finally, the algorithm employed in our 3D fluid code ensures conservation of total energy and mean fluid density per unit time in the absence of charge exchange and external random forcing, and it is massively parallelized using message passing interface (MPI) libraries to facilitate higher resolution. The conserved quantities, described in section 2, are used to monitor the numerical accuracy of our 3D quantum fluid plasma code. The time step during the numerical integration varies between 10^{-3} and 10^{-4}. The code uses usual 2/3 dealiasing of the Fourier modes, such that the largest k is determined typically by $k_{max} = (2/3)(1/2)N$, where N is the total number of modes in each direction. The time step used in our 3D simulations not only preserves the conserved quantities, but it also minimizes the aliasing errors.

The localized initial turbulent spectral distribution, concentrated at the lower wavenumbers, evolves in time following 3D nonlinear electron plasma wave interactions. Since the initial energy is localized in the large-scale fluctuations, the latter drive turbulent processes through migration of energy towards relatively small scales. Consequently, larger eddies transfer their energy to smaller ones through a forward cascade. During the forward cascade process, each Fourier mode in the inertial range spectrum obeys the vector triad constraints [23] imposed by the vector relation $\mathbf{k} + \mathbf{p} = \mathbf{q}$. These nonlinear interactions involve the neighboring Fourier components ($\mathbf{k}$, $\mathbf{p}$, $\mathbf{q}$) that are excited in the local inertial range turbulence. We have performed a number of simulations to verify the consistency of our results in a strong turbulence regime. In our 3D simulations, we have explored two dense plasma systems that are characterized by different physical parameters, viz dense warm plasmas in the next generation laser-based plasma compression (LBPC) schemes [31], and the superdense astrophysical bodies [33] (e.g. interior of white dwarf stars). It is expected that in the LBPC schemes, the electron number density

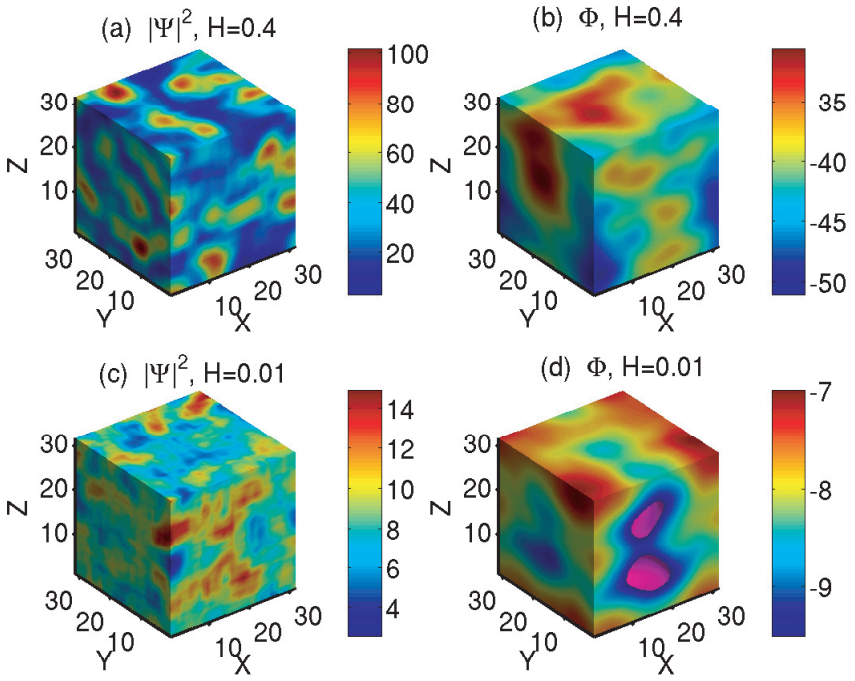

Figure 1. Fluctuations in the electron number density resulting from a steady-state turbulence simulations of our 3D electron quantum plasma. Forward cascades are responsible for the generation of relatively small-scale fluctuations in a decaying 3D electron quantum plasma as shown in (a). Large-scale electron flow structures are present in the ES potential, essentially resulting from a merging of smaller scale fluctuations as shown in (b). The latter is known as the inverse cascade process. $H = 0.4$ is used in (a) and (b), (c) and (d) depict the electron number density and the ES potential for $H = 0.01$.

may reach $10^{33}\,\mathrm{m}^{-3}$ and beyond. Hence, we have $\Omega_{\mathrm{pe}} = 1.76 \times 10^{18}\,\mathrm{s}^{-1}$, $k_{\mathrm{B}}T_{\mathrm{F}} = 1.7 \times 10^{-16}\,\mathrm{J}$, $\hbar\Omega_{\mathrm{pe}} = 1.7 \times 10^{-16}\,\mathrm{J}$ and $H = 1$. The Fermi–Debye radius $\lambda_{\mathrm{D}} = 0.1\,\text{Å}$. On the other hand, in the interior of white dwarf stars, we typically have $n_0 \sim 10^{36}\,\mathrm{m}^{-3}$ (such values are also common in dense neutron stars and supernovae), yielding $\Omega_{\mathrm{pe}} = 5.64 \times 10^{19}\,\mathrm{s}^{-1}$, $k_{\mathrm{B}}T_{\mathrm{F}} = 1.7 \times 10^{-14}\,\mathrm{J}$, $\hbar\Omega_{\mathrm{pe}} = 5.64 \times 10^{-15}\,\mathrm{J}$, $H \approx 0.3$ and $\lambda_{\mathrm{D}} = 0.025\,\text{Å}$. The numerical solutions of equations (1) and (2) for $H = 0.4$ and 0.025 (corresponding to $n_0 = 10^{33}$ and $10^{36}\,\mathrm{m}^{-3}$, respectively) are displayed in figure 1, which are the electron number density (left figures) and ES potential distributions (right figures) in the (x, y, z)-cube.

One of the most notable features of our simulations encompassing 3D electron fluid turbulence is that it exhibits a dual cascade phenomenon, as shown in figure 1. The electron density distribution in figure 1 shows a tendency to generate smaller length-scale structures, whereas the ES potential cascades toward larger scales. The co-existence of smaller and larger scale structures in turbulence is a ubiquitous feature of various 2D and 3D turbulence systems. For example, in 2D hydrodynamic turbulence, the incompressible fluid admits two invariants, namely the energy and the mean squared vorticity. The two invariants, under the action of an external forcing, cascade simultaneously in turbulence, thereby leading to a dual cascade

phenomenon. On the other hand, 3D MHD turbulence exhibits forward cascades of energy and an inverse cascade of magnetic helicity. In these processes, the energy cascades toward smaller length-scales, whereas the magnetic helicity in MHD transfer spectral power toward larger length-scales. By contrast, the fluid vorticity in 3D hydrodynamics is prohibited from an inverse cascade. The randomly excited 3D Fourier modes nonetheless transfer the spectral energy by conserving the constants of motion in k-space. In freely decaying quantum electron fluid turbulence reported here, the energy contained in the large-scale eddies is transferred to the smaller scales, leading to a statistically stationary inertial regime associated with the forward cascades of one of the invariants. Decaying turbulence often leads to the formation of coherent structures as turbulence relaxes, thus making nonlinear interactions rather inefficient when they are saturated. It is to be noted further that the long-scale flow generation in our 3D simulations is observed to be directly proportional to the parameter H. Intermittent flows are thus generated for a small value of H, whereas strong and large scale flows in the ES potential are formed when the magnitude of H is large (see, e.g. figure 1). The physical basis of this observation can be elucidated from the following arguments. The parameter H, which is the ratio between the energy density of the EPOs and the electron kinetic energy density of a warm dense quantum plasma, is associated with a diffraction-like term in equation (1), i.e. $H\nabla^2\Psi$. In this term, the negative imaginary part of the complex evolutionary variable Ψ essentially determines the rate of dissipation corresponding to the smaller scales. The smaller H is, the more the dissipation is concentrated at the smaller scales and vice versa. For a moderately higher magnitude of the H parameter, there exists a strong tendency in EPOs to dissipate the smaller and intermittent turbulent eddies. It is therefore this H parameter which essentially characterizes electron flows at nanoscales in our 3D simulations.

While the power spectrum for nonlinear EPOs exhibits an interesting feature in our 3D simulations, its scaling is not universal and is determined critically by the parameter H. For instance, we find a 3D Kolmogorov-like power spectrum $k^{-11/3}$ in some range of H values as shown in figure 2. The corresponding omnidirectional spectrum thus exhibits a $k^{-5/3}$ scaling. Spectral index nevertheless changes with H, as noted also in the study of 2D fluid turbulence [17]. However, the spectral slope in the latter was found to be close to the Iroshnikov–Kraichnan (IK) power law [34, 35] $k^{-3/2}$, rather than the usual Kolomogrov scaling [36] $k^{-5/3}$. The origin of the differences in the observed spectral indices resides with the nonlinear character of the underlying warm dense plasmas, as nonlinear interactions in the 2D and 3D systems are governed typically by different nonlinear forces. The latter modify the spectral evolution of turbulent cascades to a significant degree.

4. Electron transport caused by turbulent fields

We finally study the electron diffusion coefficient in the presence of small- and large-scale turbulent EPOs. The effective electron diffusion coefficient produced by the momentum transfer can be calculated from $D_{\rm eff} = \int_0^\infty \langle \mathbf{P}(\mathbf{r}, t) \cdot \mathbf{P}(\mathbf{r}, t + t') \rangle \, {\rm d}t'$, where $\mathbf{P}$ is the electron momentum and the angular bracket denotes spatial averages and the ensemble averages are normalized to unit mass. The effective diffusion coefficient $D_{\rm eff}$, resulting from 3D structures, essentially relates the diffusion processes associated with random translational motions of electrons in nonlinear fields of localized EPOs. It is *remarkable* to note that the electron transport can be effectively suppressed when the magnitude of the parameter H is decreased. This is shown in figure 3. The outcome of figure 3 is contrary to our 2D results [17], where the effective

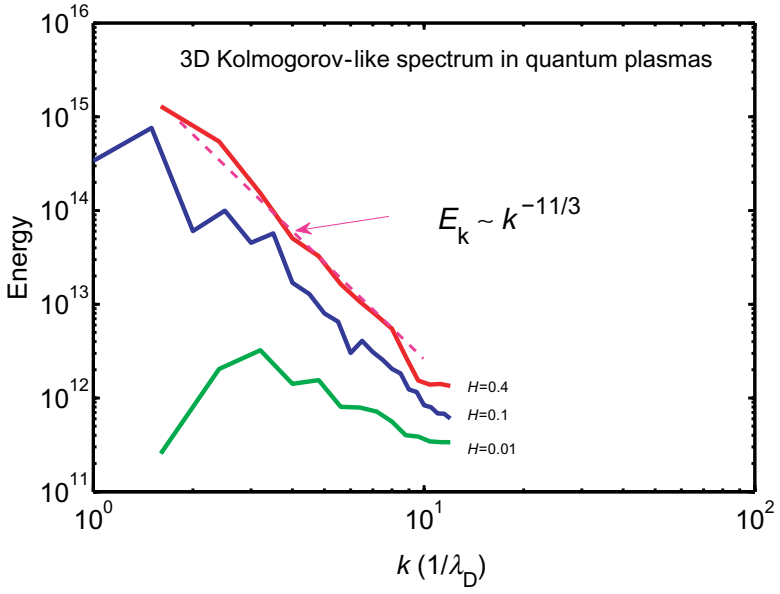

Figure 2. Energy spectrum of 3D EPOs in a forward cascade regime. A Kolmogorov-like $k^{-11/3}$ has been observed for $H = 0.4$. The spectral index changes with respect to the parameter H. Numerical resolution is 128^3.

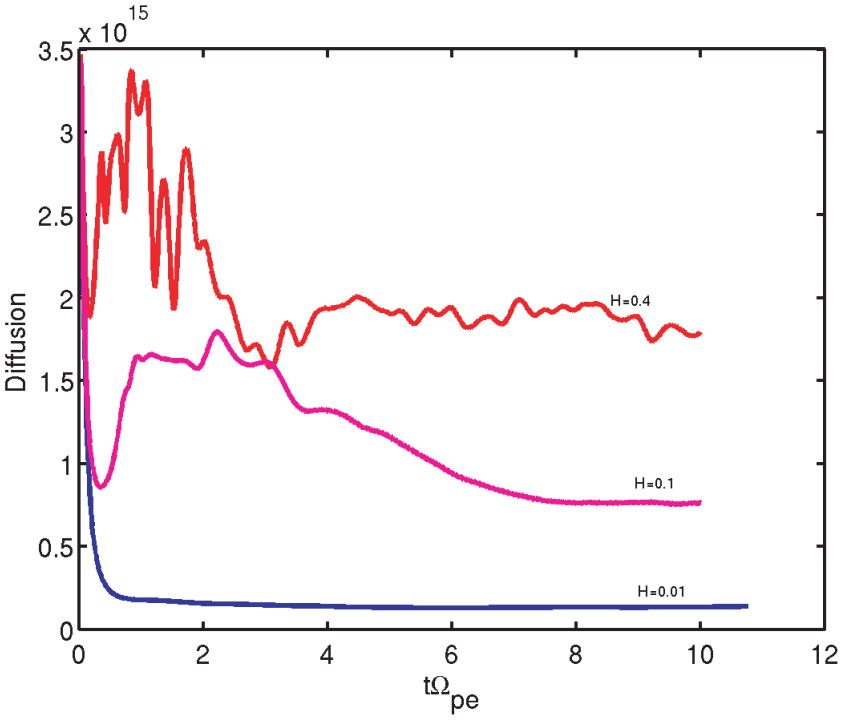

Figure 3. Time evolution of effective electron diffusion coefficients measured for different values of H. Interestingly, smaller values of H corresponds to an effective low-diffusion coefficient. The latter characterizes the presence of small-scale turbulent eddies which results in suppression of the electron transport.

electron diffusion was lower when the field perturbations were Gaussian and increases later rapidly with the eventual formation of longer length-scale structures. Unlike the 2D case, the electron diffusion in the 3D case is suppressed eventually because of the presence of small-scale turbulent fluctuations. However, the steady-state diffusion coefficient increases with the increase of H. This can be understood as follows. The higher the H values, the stronger the small-scale damping. When the small-scale fluctuations are smeared out, the dynamical evolution of 3D quantum electron plasma wave turbulence is predominantly governed by the large scale flows, which consequently lead to a higher level of transport. This finding is further consistent with the fact that the parameter H dictates the characteristic evolution properties of the 3D EPOs, as described above.

5. Summary

In conclusion, we have presented results from 3D nonlinear fluid simulations of the electron fluid turbulence at nanoscales in an unmagnetized warm dense plasma. The mode couplings between the electron wave function and the ES potential associated with the underlying EPOs lead to the onset of nonlinear interactions and subsequent cascades in the inertial range. We find from our 3D simulations that the dispersion effect associated with the quantum Bohm potential plays a critical role in determining the inertial range turbulent spectrum and the subsequent transport level exhibited by the 3D EPOs. For instance, a Kolmogorov-like $k^{-11/3}$ 3D spectrum is observed for $H = 0.4$, whereas the spectrum flattens out for a smaller value of H. Correspondingly, the electron transport is higher for the higher H values. Finally, the wave function cascades toward smaller length scales, while the ES potential follows an inverse cascade. We reiterate that the present investigation of 3D EPO turbulence is a necessary prerequisite for understanding the complex dynamical phenomena occurring at nanoscales in warm dense plasmas, such as those in laboratory and astrophysical settings.

References

[1] Barnes W L, Dereux A and Ebbesen T W 2003 Surface plasmon subwavelength optics *Nature* **424** 824
[2] Marklund M, Brodin G, Stenflo L and Liu C S 2007 New quantum limits in plasmonic devices *Preprint* 0712.3145v1
[3] Maier S A 2007 *Plasmonics* (Berlin: Springer)
[4] Chang D E, Sorensen A S, Demler E A and Lukin M D 2007 A single-photon transistor using nano-scale surface plasmons *Nat. Phys.* **3** 807
[5] Pitarke J M, Silkhon V M, Chulikov E V and Echenique P M 2007 Theory of surface plasmons and surface-plasmon polaritons *Rep. Prog. Phys.* **70** 1
[6] Markowich P A, Ringhofer C A and Schmeiser C 1990 *Semiconductor Equations* (Berlin: Springer)
[7] Craighead H C 2000 Nanoelectromechanical systems *Science* **290** 1532
[8] Ang L K and Zhang P 2007 Ultrashort-pulse Child–Langmuir law in the quantum and relativistic regimes *Phys. Rev. Lett.* **98** 164802
[9] Lee M, Im J, Lee B Y, Myung S, Kang J, Huang L, Kwon Y K and Hong S 2006 Linker-free directed assembly of high performance integrated devices based on nanotubes and nanowires *Nat. Nanotechnol.* **1** 66
[10] Serbeto A, Mendonça J T, Tsui K H and Bonifacio R 2008 Quantum wave kinetics of high-gain free electron lasers *Phys. Plasmas* **15** 013110
[11] Chabrier G, Saumon D and Potekhin A Y 2006 Dense plasmas in astrophysics: from giant planets to neutron stars *J. Phys. A: Math. Gen.* **39** 4411

[12] Harding A K and Lai D 2006 Physics of strongly magnetized neutron stars *Rep. Prog. Phys.* **69** 2631
[13] Glenzer S H *et al* 2007 Observation of plasmons in warm dense matter *Phys. Rev. Lett.* **98** 065002
[14] Gardner C L and Ringhofer C 1996 Smooth quantum potential for the hydrodynamic model *Phys. Rev.* E **53** 157
[15] Marklund M and Brodin G 2007 Dynamics of spin-1/2 quantum plasmas *Phys. Rev. Lett.* **98** 025001
[16] Shukla P K and Eliasson B 2006 Formation and dynamics of dark solitons and vortices in quantum electron plasmas *Phys. Rev. Lett.* **96** 245001
[17] Shaikh D and Shukla P K 2007 Fluid turbulence in quantum plasmas *Phys. Rev. Lett.* **99** 125002
[18] Shukla P K and Eliasson B 2007 Nonlinear interactions between electromagnetic waves and electron plasma oscillations in quantum plasmas *Phys. Rev. Lett.* **96** 096401
[19] Pines D 1961 Quantum plasma physics. *J. Nucl. Energy: Part C: Plasma Phys.* **2** 5
[20] Zakharov V E 1972 Collapse of Langmuir waves *Sov. Phys.—JETP* **62** 908
[21] Goldman M V 1984 Strong turbulence of plasma waves *Rev. Mod. Phys.* **66** 709
[22] Sulem C and Sulem P L 1999 *The Nonlinear Schrödinger Equations* (New York: Springer) chapter 13 pp 346–60
[23] Murtaza G and Shukla P K 1984 Nonlinear generation of electromagnetic waves in a magnetoplasma *J. Plasma Phys.* **31** 423
[24] Lesieur M 1990 *Turbulence in Fluids* (Dordrecht: Kluwer)
[25] Frisch U 1995 *Turbulence* (Cambridge: Cambridge University Press)
[26] Horton W and Hasegawa A 2004 Quasi-two-dimensional dynamics of plasmas and fluid *Chaos* **4** 227
[27] Hasegawa A 1985 Self-organization processes in continuous media *Adv. Phys.* **34** 1
[28] Kobayashi M and Tsubota M 2005 Kolmogorov spectrum of superfluid turbulence: numerical analysis of the Gross–Pitaevskii equation with a small dissipation *Phys. Rev. Lett.* **94** 065302
[29] Kobayashi M and Tsubota M 2006 Thermal dissipation in quantum turbulence *Phys. Rev. Lett.* **97** 145301
[30] Manfredi G 2005 How to model quantum plasmas *Fields Inst. Commun.* **46** 263
[31] Malkin V M, Fisch N J and Wurtle J S 2007 Compression of powerful x-ray pulses to attosecond by stimulated Raman backscattering in plasmas *Phys. Rev.* E **75** 026404
[32] Gottlieb D and Orszag S A 1977 *Numerical Analysis of Spectral Methods* (Philadelphia: SIAM)
[33] Harding A K and Lai D 2006 Physics of strongly magnetized neutron stars *Rep. Prog. Phys.* **69** 2631
[34] Kolmogorov A N 1941 The local structure of turbulence in incompressible viscous fluid for very large Reynolds' numbers *C. R. Acad. Sci. USSR* **30** 301
[35] Iroshnikov P 1963 Turbulence of a conducting liquid in a strong magnetic field *Sov. Astron.* **7** 566
[36] Kraichnan R H 1965 Inertial-range spectrum of hydromagnetic turbulence *Phys. Fluids* **8** 1385